Silica-Gel-Confined Ionic Liquids: A New Attempt for the Development of Supported Nanoliquid Catalysis

Feng Shi, Qinghua Zhang, Dongmei Li, and Youquan Deng*[a]

Abstract: A new concept of designing and synthesizing highly dispersed ionic-liquid catalysts was developed through physical confinement or encapsulation of ionic liquids (with or without metal complex) in a silica-gel matrix through a sol–gel process. We studied ionic liquids such as $EMImBF_4$, $BuMImBF_4$, $DMImBF_4$, $CMImBF_4$, $BuMImPF_6$, either with or without $[Pd(PPh_3)_2Cl_2]$ and $[Rh(PPh_3)_3Cl]$, in a silica-gel matrix (E = ethyl, Bu = butyl M = methyl, D = decyl, C = cetyl and Im = imidazolium). The contents of ionic liquids and loadings of Pd or Rh were 8–53 wt% and 0.1~0.15 wt%, respectively. Analyses of FT-Raman spectra showed that abnormal Raman spectra of the confined ionic liquids were observed in comparison with the bulk and pure ionic liquids. $EMImBF_4$ and $BuMImBF_4$ ionic liquids could be completely washed out from the silica-gel matrix under vigorous reflux conditions, but ionic liquids with larger molecular size, for example, $DMImBF_4$ or $CMImBF_4$, could be confined into the silica-gel nanopores relatively firmly. These results suggested that the ionic liquids were physically confined or encapsulated into the silica gel. The N_2 adsorption measurements indicated that the silica-gel skeleton was mesoporous with 50–110 Å pore size after the $BuMImBF_4$ ionic liquid was removed completely. Transmission electron microscopy (TEM) and X-ray diffraction (XRD) analysis showed that the silica-gel matrix was amorphous and non-uniformly mesoporous. Carbonylation of aniline and nitrobenzene for synthesis of diphenyl urea, carbonylation of aniline for synthesis of carbamates, and oxime transformation between cyclohexanone oxime and acetone were used as test reactions for these catalysts. Catalytic activities were remarkably enhanced with much lower amounts of ionic liquids needed with respect to bulk ionic-liquid catalysts or silica-supported ionic-liquid catalysts prepared with simple impregnation, in which the ionic liquid may be deposited as a thin layer on the support. Such unusual enhancement in catalytic activities may be attributed to the formation of nanoscale and high-concentration ionic liquids due to the confinement of the ionic liquid in silica gel; this results in unusual changes in the symmetry and coordination geometry of the ionic liquids.

Keywords: carbonylation · catalysis · ionic liquids · nanotechnology · synthesis design

Introduction

Supported solid nanocatalysis has been the subject of enormous interest in catalysis science and technology, because of its potential and wide-ranging applications in the chemical industry and environmental protection.[1,2] In previous studies and applications, supported solid nanocatalysts were basically metals, oxides, or zeolites; that is, the catalytically active nanomaterials were all macroscopic solids. A typical representation of supported solid nanocatalysts would be metal oxides or polymer-supported Au nanocatalysts, which have exhibited high catalytic activity for CO oxidation or carbonylations.[3–5]

On the other hand, homogeneous or liquid-phase catalysts offer a number of important advantages; for example, all catalytically active sites are accessible and uniform. Usually, solvents are indispensable as reaction media and have even played an important role in efficient homogeneous catalysis. Different or unexpected catalytic performance may occur if a bulk homogeneous catalyst system, that is, a reaction medium plus metal complex catalyst, is highly dispersed on the nanoscale. Nanoliquid catalyst production has not yet been reported in the literature, probably because of difficulties in obtaining stable nanoliquid catalysts due to the volatility of ordinary organic solvents as reaction media for the

[a] Dr. F. Shi, Q. Zhang, D. Li, Prof. Y. Deng
Center for Green Chemistry and Catalysis
Lanzhou Institute of Chemical Physics
Chinese Academy of Sciences, Lanzhou, 730000 (China)
Fax: (+86) 931-496-8116
E-mail: ydeng@lzb.ac.cn

 DOI: 10.1002/chem.200500107 © 2005 Wiley-VCH Verlag GmbH & Co. KGaA, Weinheim

metal complex catalyst. However, some studies on confined nanoliquids have been reported recently.[6–8]

Though not new, room-temperature ionic liquids have received much attention as being potentially environmentally benign or as suitable reaction media for organic syntheses, nanosolid catalysts,[9–16] and as novel liquid catalysts.[17–26] Their favorable properties, such as thermal stability, negligible vapor pressure, peculiar ion environment, and diversity, may provide good opportunities to develop new kinds of supported nanoliquid catalyst systems. Here, an attempt has been made to confine ionic liquids either with or without metal complex, into the nanopores of solid silica gel with a "one-pot assembly" of ionic liquid (or ionic liquid plus metal complex) and silicate ester through a sol–gel process. Under these conditions, a new kind of mesoporous silica-gel-supported ionic-liquid nanocatalyst could be established, since ionic liquids could also be used as appropriate templates to prepare nanostructured materials.[27,28] The key concept of designing and synthesizing such a catalyst system involves the physical confinement or encapsulation of ionic liquid (either with or without metal complex) through a traditional sol–gel process, based on the hydrolysis of silicate esters to produce a solid matrix with desired pore sizes or cavities and channels. The ionic liquid acts as both catalyst and reaction media, and the solid matrix acts as the nanoscale reactor connected with inlets and outlets to contain the ionic liquid and metal complex and to allow reactants and products to be transported in or out. The pore size of the nanoreactor should be large enough to contain ionic liquids, while the channel size of the nanoreactor should be small enough to prevent ionic liquids or metal complex from leaching; however, the channel size must also be large enough for free transportation of reactant and product, (Figure 1). Therefore, they are intrinsically different from previously reported supported or immobilized ionic-liquid catalysts,[28–30] in which the ionic-liquid fragment, such as the dialkyl imidazolium cation, was covalently bound to the silica surface or immobilized by dipping the porous support in the ionic liquid containing the metal complex. Chemical bonding of the dialkyl imidazolium cation to a solid surface, however, may limit the degrees of freedom of the dialkyl imidazolium cation and even change the physicochemical properties of the ionic liquids. Hence the leaching of the ionic liquids and metal-complex catalyst was unavoidable under rigorous reaction conditions if the supported ionic-liquid catalyst was prepared by physical adsorption or by having the ionic liquid as a thin layer on a support material.

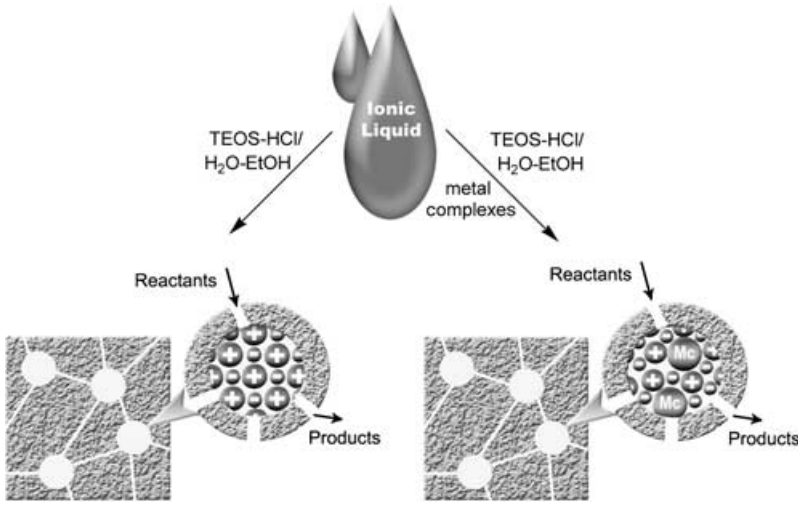

Figure 1. Illustration of the synthesis of silica-gel-confined ionic liquids with and without the metal complex (Mc).

Results and Discussion

FT-Raman characterization of silica-gel-confined ionic-liquid catalysts: Since the concentration of metal complex in the silica-gel-confined ionic-liquid catalysts was too low to be detected in the FT-Raman spectrometer, only the samples of silica-gel-confined ionic liquid without the metal complex are shown here. $BuMImBF_4$/silica gel and $DMImBF_4$/silica gel (Scheme 1) with different ionic liquid

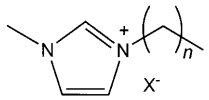

Scheme 1. General structure for the ionic liquids. X = BF_4: $n=1$ $EMImBF_4$, $n=3$ $BuMImBF_4$, $n=9$ $DMImBF_4$, $n=15$ $CMImBF_4$; X = PF_6: $n=3$ $BuMImPF_6$. E = Ethyl; M = Methyl; Im = imidazolium; Bu = Butyl; D = Decyl; C = Cetyl.

loadings were firstly characterized with FT-Raman spectroscopy, Figures 2 and 3. The results revealed that the Raman spectra at 8–53 wt % Bu(or D)$MImBF_4$/silica gel samples were different from pure bulk ionic liquids, that is, abnormal FT-Raman spectra were observed. In comparison with corresponding bulk ionic liquids, the bands at 2967, 1421, and 766 cm^{-1} for $BuMImBF_4$ (or 2898, 1421, 1025, and 766 cm^{-1} for $DMImBF_4$), which may be attributable to several skeletal modes of the side alkyl chains of imidazolium,[31–34] were remarkably inhibited, or even disappeared and then reappeared, with increasing loading of the ionic liquids. At the same time, bands at 2941, 1449, and 880 cm^{-1} for $BuMImBF_4$ (or 2930, 1453, and 879 cm^{-1} for $DMImBF_4$), which may be attributable to several skeletal modes of the imidazolium ring, appeared or strengthened, and then disappeared or weakened again, when the loadings of confined

© 2005 Wiley-VCH Verlag GmbH & Co. KGaA, Weinheim

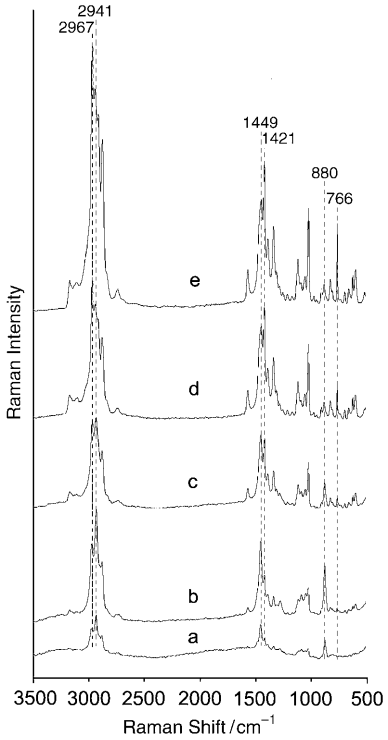

Figure 2. FT-Raman spectra of pure $BuMImBF_4$ and $BuMImBF_4$/silica gel with different ionic liquid loadings: a) 8 wt%, b) 17 wt%, c) 35 wt%, d) 53 wt%, and e) pure $BuMImBF_4$.

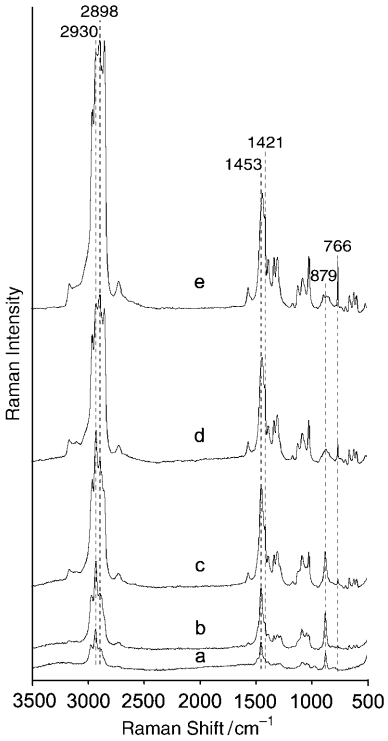

Figure 3. FT-Raman spectra of pure $DMImBF_4$ and $DMImBF_4$/silica gel with different ionic liquid loadings: a) 8 wt%, b) 17 wt%, c) 35 wt%, d) 53 wt%, and e) pure $DMImBF_4$.

ionic liquids were increased from 8 and 17 wt% and then to 35 and 53 wt%. It is worth noting that such unusual spectral peaks were much stronger when the loadings of confined ionic liquids ranged from 8 to 17 wt%, and such aberration became small and then reverted back to the same or normal spectral peaks as the bulk ionic liquids when the loadings of confined ionic liquids were further increased to 53 wt%. Unusual FT-Raman spectra similar to those for $BuMImBF_4$/silica gel were also observed for 17 wt% $EMImBF_4$/silica gel, 17 wt% $CMImBF_4$/silica gel (Figure 4), and 17 wt% $BuMImPF_6$/silica gel samples (though not shown here; see

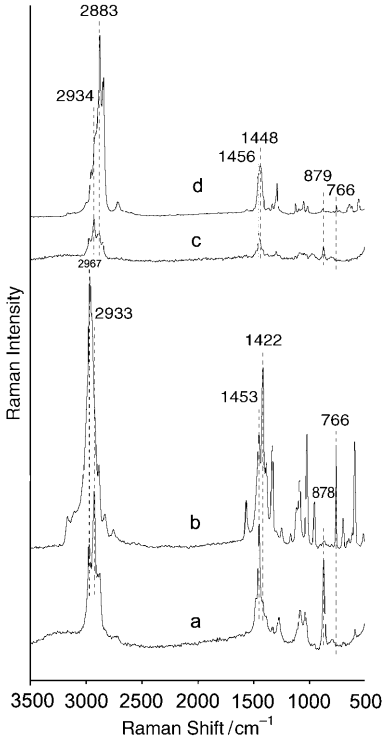

Figure 4. FT-Raman spectra of a) 17 wt% $EMImBF_4$/silica gel, b) pure $EMImBF_4$, c) 17 wt% $CMImBF_4$/silica gel, and d) pure $CMImBF_4$.

Scheme 1 for structures of these ionic liquids). This suggests that such aberration in the Raman spectra may be mainly related to skeletal-mode modification of the imidazolium ring, since variations in side-chain length of imidazolium or in anions have less impact on such phenomena.

To investigate the stability of the ionic liquids confined in silica gel, the prepared samples in which the ionic liquids had different lengths of side chain attached to the imidazolium group were washed in acetone (30 mL) under vigorous reflux at 60 °C for 3 h. This was done because $BuMImBF_4$, $DMImBF_4$, $CMImBF_4$, and $BuMImPF_6$ ionic liquids are completely soluble in acetone at this temperature. Then FT-Raman analysis was conducted (Figure 5). It can be seen that ionic liquids $DMImBF_4$ and $CMImBF_4$, which have longer side chains, could be firmly confined into the silica gel, while $BuMImBF_4$ with shorter side chains was, since the Raman spectral peaks of $DMImBF_4$ and $CMImBF_4$ re-

 © 2005 Wiley-VCH Verlag GmbH & Co. KGaA, Weinheim

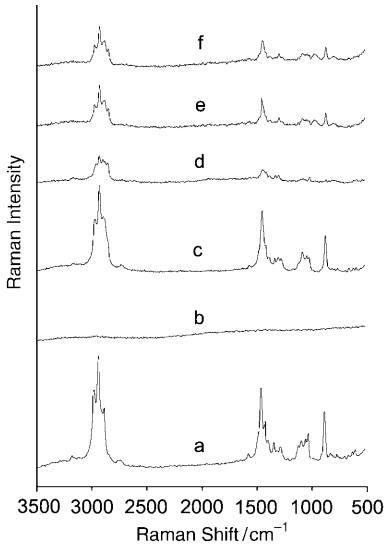

Figure 5. FT-Raman spectra of 17 wt % B(or D/C)MImBF$_4$/silica gel before and after washing. a),b) 17 wt % BuMImBF$_4$/silica gel before and after washing; c),d) 17 wt % DMImBF$_4$/silica gel before and after washing; e),f) 17 wt % CMImBF$_4$/silica gel before and after washing.

mained, while those of BuMImBF$_4$ disappeared almost completely after these samples were washed under the above-mentioned conditions. Since CMImBF$_4$ and DMImBF$_4$ ionic liquids are completely soluble in acetone at 60 °C, the fact that they could not be washed out from the silica gel should not be attributed to their lower solubility in acetone. This may also imply that there was no chemical bonding between the silica-gel surface and ionic liquid fragments, that is, the ionic liquids were physically confined or encapsulated into the silica gel, and porous materials of silica gel may be produced if the confined ionic liquids or liquids acting as a "template" were removed completely.

BET characterization of the silica-gel matrix: A porous silica-gel matrix could be formed if the confined ionic liquids with a smaller relative molecular size, such as BuMImBF$_4$, could be removed without destroying the remaining skeleton of silica gel. N_2 adsorption measurements, which have been a powerful tool for nano- or mesoporous material characterization,[35–37] were performed to attain more insight of the porous silica gels prepared by using ionic liquids as templates. Since DMImBF$_4$ or CMImBF$_4$ were confined into the pores of silica gel relatively firmly and could not be washed out in acetone under vigorous refluxing, the accurate data of average pore volume and diameter of the silica-gel matrix containing DMImBF$_4$ and CMImBF$_4$ are not available. We only measured the remaining skeleton of silica gel in which BuMImBF$_4$ and BuMImPF$_6$ ionic liquids were confined at different loadings ranging from 0–53 wt %. For the skeletons of silica gel which had originally contained confined BuMImBF$_4$ ionic liquid, the isotherm plots showed distinct hysteresis loops, whereas isotherm plots of silica gel prepared without any ionic liquid involvement indicated the formation of the typical structures of mesoporous materials (Figure 6). The BET surface areas were decreased from 933 to 322 m^2 g^{-1}, but the average pore volume and average pore diameters increased from 0.298 to 1.35 cm^3 g^{-1} and 29 to 109 Å, respectively, when amounts of confined ionic liquids were increased from 0 to 53 wt % (Table 1). Furthermore, it can be seen that the pore-size distributions were quite narrow and then became wider when the amounts of confined BuMImBF$_4$ ionic liquid was below 35 wt % or near to 53 wt %, respectively; this suggests that ionic liquids may be well confined in the pores of silica gel when the loadings of ionic liquids were lower than 35 wt %. In the case of silica-gel-confined BuMImPF$_6$, mesoporous silica gel was also obtained when the ionic liquid was removed (Figure 7), but the corresponding average pore diameters were much larger (168 and 343 Å) and the pore-size distribution became quite wide relative to that of BuMImBF$_4$/silica gels (42 and 71 Å and a relatively narrow pore-size distribution) when the same amount of ionic liquids by weight were confined.

TEM and XRD analysis: We analyzed pure silica gel (that is 0 wt % ionic liquid loading) and 17 wt % DMImBF$_4$/silica gel by high-resolution transmission electron microscopy (HRTEM), see Figure 8. Uniform but amorphous textures were observed for both the pure silica gel and silica-gel-confined ionic liquids. Unfortunately, the "particles" of ionic liquid over or in the silica gel were not visible, since the ionic liquid could not be distinguished from the silica gel substrate. Although not shown here, XRD results of pure silica gel, 17 wt % BuMImBF$_4$/silica gel, and 17 wt % DMImBF$_4$/silica gel showed that the structures of silica gel and the ionic liquids were amorphous.

Based on the results of FT-Raman spectroscopy, N_2 adsorption measurements, TEM and XRD analysis, some insight into the silica-gel-confined ionic liquids could be gained.

1) the size of particles of ionic liquids confined in the silica-gel matrix may range into the nanoscale; for example, ionic-liquid particles 40–110 Å in diameter may be formed over 7–53 wt % BuMImBF$_4$/silica gel.
2) The unusual FT-Raman spectra could be attributed to the nanoeffect; that is, changes in the ionic liquid symmetry and unusual coordination geometry occurred when ionic liquids were confined or encapsulated into the nanopores of silica gel.[38–41] Also, unusual FT-Raman spectra showing strong peaks occurred when the amount of confined ionic liquids was about 17 wt %.
3) The fact that BuMIm cations could move in the channels easily but DMIm and CMIm cations could not suggested that the silica-gel matrices containing BuMImBF$_4$ and DMImBF$_4$ may possess similar sizes of channels, although the pore-size distributions of silica gel matrices containing DMImBF$_4$ were unknown.
4) The particle sizes of DMImBF$_4$ and CMImBF$_4$ in DMIm(or CMIm)BF$_4$/silica gels, though not derivable through N_2 adsorption measurement, should also be in

© 2005 Wiley-VCH Verlag GmbH & Co. KGaA, Weinheim

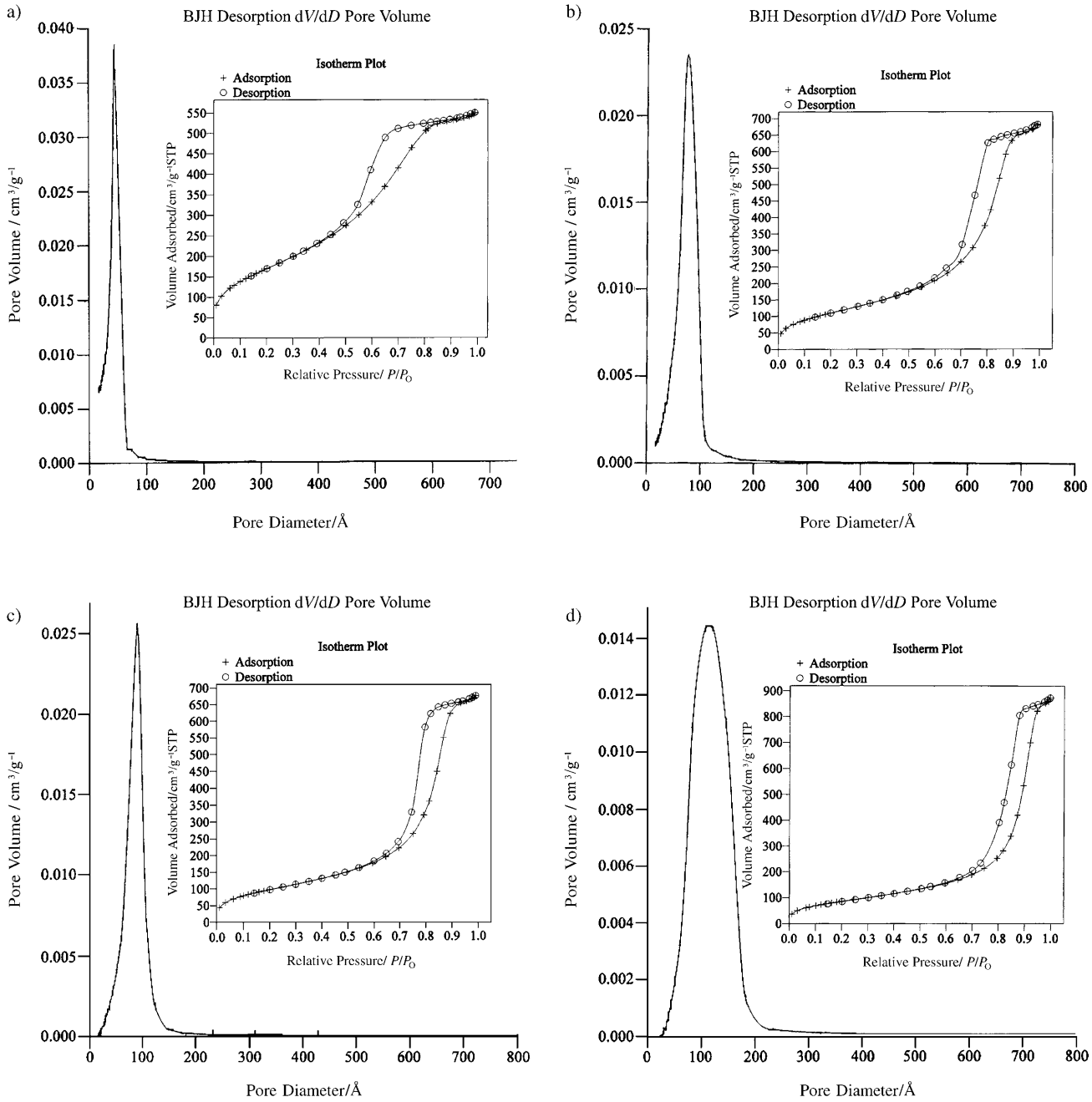

Figure 6. Pore-size distribution and N_2 adsorption–desorption isotherms of silica gel matrices after the confined $BuMImBF_4$ was removed: a) silica gel skeleton from 8 wt % $BuMImBF_4$/silica gel, b) silica gel skeleton from 17 wt % $BuMImBF_4$/silica gel, c) silica gel skeleton from 35 wt % $BuMImBF_4$/silica gel, and d) silica gel skeleton from 53 wt % $BuMImBF_4$/silica gel.

Table 1. Results of N_2 adsorption measurements of the remaining skeletons of silica gel after being washed to remove confined $BuMImBF_4$ and $BuMImPF_6$ ionic liquids.

Original samples	BET surface area [m^2g^{-1}]	Single desorption pore volume [cm^3g^{-1}]	BJH desorption average pore diameter [Å]
pure silica gel	933	0.298	29
8 % $BuMImBF_4$/silica gel	634	0.878	42
17 % $BuMImBF_4$/silica gel	415	1.059	71
35 % $BuMImBF_4$/silica gel	360	1.044	81
53 % $BuMImBF_4$/silica gel	322	1.35	109
8 % $BuMImPF_6$/silica gel	212	1.32	168
17 % $BuMImPF_6$/silica gel	108	1.15	343

 © 2005 Wiley-VCH Verlag GmbH & Co. KGaA, Weinheim

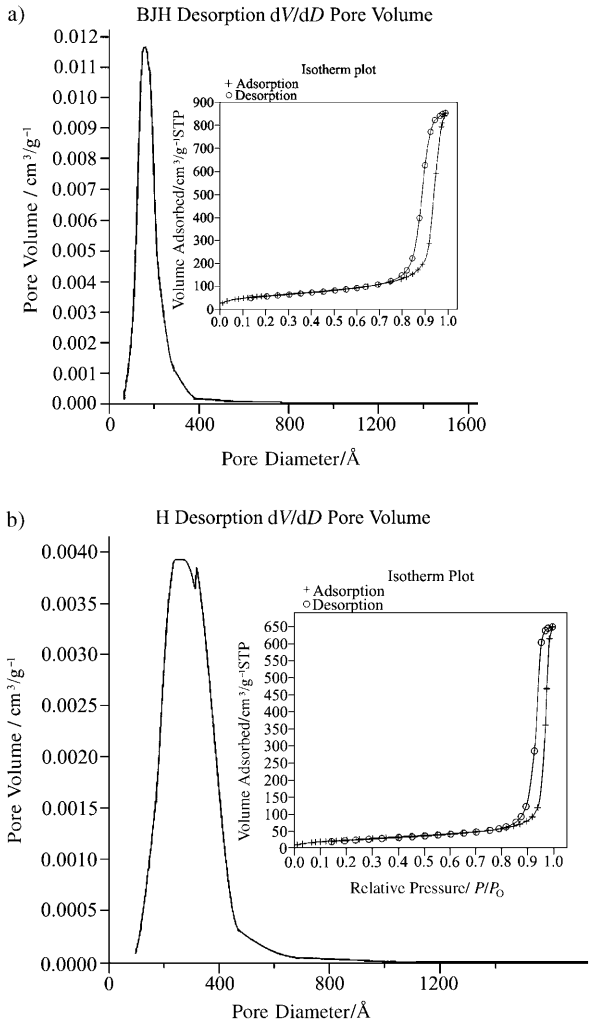

Figure 7. Pore-size distribution and N_2 adsorption–desorption isotherms of silica gel matrices after the confined $BuMImPF_6$ was removed: Top: silica gel skeleton from 8 wt % $BuMImPF_6$/silica. Bottom: silica gel skeleton from 17 wt % $BuMImPF_6$/silica gel.

the nanoscale range, since very similar unusual FT-Raman spectra were exhibited.

5) Non-uniform mesoporous silica gels confined with nanoscale ionic-liquid particles were formed.

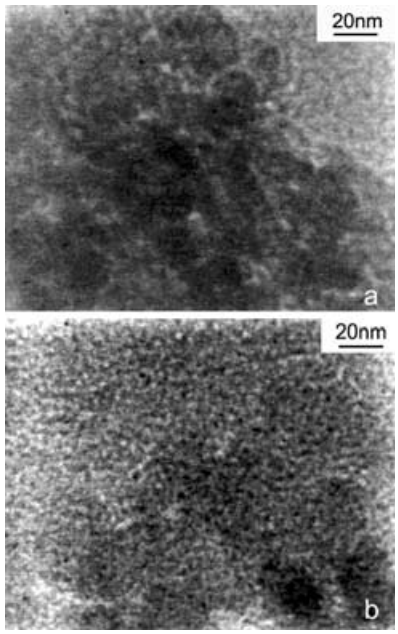

Figure 8. TEM pictures of a) pure silica gel and b) 17 wt % $DMImBF_4$/silica gel.

Synthesis of diphenyl urea: Carbonylation of aniline and nitrobenzene for the synthesis of diphenyl is an important process that generally proceeds in the presence of a suitable noble-metal complex as catalyst. For the purpose of comparison, $[Rh(PPh_3)_3Cl]$ only, physical mixtures of $DMImBF_4$/silica gel, and $[Rh(PPh_3)_3Cl]$/$DMImBF_4$/silica gel as catalysts were examined first (Table 2, entries 1–3). Poor catalytic performances were observed over these catalysts. However, the carbonylation of aniline and nitrobenzene proceeded efficiently over Rh- (or Pd)–D(or E)$MImBF_4$/silica gel as catalysts with conversions of 81–93 % and selectivity >98 % (Table 2, entries 4–6). The best catalytic performance was achieved over Rh-$DMImBF_4$/silica gel, and the corresponding TOF exceeded 11 000 $mol\,mol^{-1}\,h^{-1}$. In comparison with the results shown in Table 2 (entries 1–3), it is worth noting that although the amount of ionic liquid used was much less, the catalytic performances were much better for the metal complex/ionic liquid/silica gel catalysts. This means that more enhanced catalytic activity was exhibited through the confinement or high concentration of an ionic liquid containing a metal complex in the pores or cavities of the silica-gel matrix; however, such an effect would disappear when the bulk ionic liquid and metal complexes were completely diluted with large amounts of the reactant molecules, thus resulting in poor catalytic performance. For the catalyst regeneration,

Table 2. Results of carbonylation of nitrobenzene and aniline to diphenyl urea.

	Catalysts	Ionic liquid/ metal complex [mg]	Conversion [%] nitrobenzene	aniline	Sel [%]	TOF[a]
1	$[Rh(PPh_3)_3Cl]$	0/1	8	9	>95	1586
2	$DMImBF_4$ + silica gel	200/0	–	–	–	–
3	$[Rh(PPh_3)_3Cl]$ + $DMImBF_4$ + pure silica gel	200/1	41	39	>98	7463
4	0.11 wt % Rh–35 wt % $DMImBF_4$/silica gel	~35/~1	93	92	>98	11 548
5	0.15 wt % Pd–35 wt % $DMImBF_4$/silica gel	~35/~1	81	79	>98	7440
6	0.13 wt % Rh–35 wt % $EMImBF_4$/silica gel	~35/~1	85	84	>98	10 550
7[b]	0.11 wt % Rh–35 wt % $DMImBF_4$/silica gel	~35/~1	83	81	>98	10 800
8[b]	0.13 wt % Rh–35 wt % $EMImBF_4$/silica gel	~35/~1	16	16	>98	9987
9	0.11 wt % Rh–35 wt % $DMImBF_4/SiO_2$	~35/~1	3	4	>98	2180

[a] TOF = mol substrates converted per mol metal complexes per hour. [b] The catalyst system had been recovered and reused for the second time.

© 2005 Wiley-VCH Verlag GmbH & Co. KGaA, Weinheim

methanol (20 mL) was added to the resultant solid mixture (if the conversion and selectivity was high enough) to dissolve the unreacted substrates from the catalyst and desired product. The mixture was filtered to remove methanol containing unreacted substrates, and water (20 mL) was added to the remaining solid mixture containing diphenyl urea and the catalyst. The diphenyl urea floats on the water surface and the catalyst is deposited on the base of the reaction vessel. Hence, they could be separated easily with a simple dredge and filtration, and the catalyst could be reused after drying. An aniline conversion of 81% and >98% selectivity were maintained when 0.11 wt% Rh-35 wt% $DMImBF_4$/silica gel was reused for the second time (Table 2, entry 7). The catalytic activity was greatly reduced when the used Rh-$EMImBF_4$/silica gel was reused for the second time (Table 2, entry 8). Analyses of Rh content in 0.11 wt% Rh-35 wt% $DMImBF_4$/silica gel and 0.13 wt% Rh-35 wt% $EMImBF_4$/silica gel after being used for twice gave results of 0.08 and 0.09 wt%, respectively. FT-Raman analyses of the ionic liquids contents in 0.11 wt% Rh-35 wt% $DMImBF_4$/silica gel and 0.13 wt% Rh-35 wt% $EMImBF_4$/silica gel before and after reaction showed that the characteristic peaks of $EMImBF_4$ had almost disappeared, whilst the characteristic peaks of $DMImBF_4$ could be observed clearly but were slightly weakened. These results suggested that the deactivation of 0.13 wt% Rh-35 wt% $EMImBF_4$/silica gel was mainly due to $EMImBF_4$ leaching from silica gel, because of its smaller molecular size rather than Rh complex leaching, while $DMImBF_4$ could be confined into the pores of silica gel relatively firmly due to its larger molecular size, thus maintaining a more stable activity. Though not shown here, carbonylation of aniline and nitrobenzene were also examined over Rh-D-(or E)$MImPF_6$/silica gels. It was found that $BuMImPF_6$ was liable to decompose in the presence of water or acid during reaction.

For the purpose of comparison, a silica-supported ionic-liquid catalyst containing $Rh(PPh_3)_3Cl$, that is, 0.11% Rh-35 wt% $DMImBF_4/SiO_2$, in which the ionic liquid was deposited only as a thin layer on the support according to the FT-Raman characterization (Figure 9), was also tested with the carbonylation of nitrobenzene and aniline to diphenyl carbonate; however, the conversions were only 3 and 4% respectively (Table 2, entry 9).

Syntheses of phenyl carbamates and oxime transformation: To examine the possible universality of such a silica-gel-confined ionic-liquid catalyst system, oxidative carbonylation of aniline to afford carbamate, a key intermediate for the nonphosgene synthesis of 4,4′-dipheylmethyldiisocyanates,[42–44] and transformation between cyclohexanone oxime and acetone were also conducted over the Rh(or Pd)-$DMImBF_4$/silica gel, $DMImBF_4$/silica gel, and 17 wt% $DMImBF_4/SiO_2$ catalysts. For oxidative carbonylation of aniline, lower catalyst activities were obtained with the bulk $DMImBF_4$ ionic liquid + $Pd(PPh_3)_2Cl_2$ or Rh-$(PPh_3)_3Cl$ catalyst system (Table 3, entries 1 and 2). Greatly enhanced catalytic activities were observed with the Pd(Rh)-35 wt% $DMImBF_4$/silica gel although the amount of ionic liquid used was greatly reduced (Table 3, entries 3 and 4).

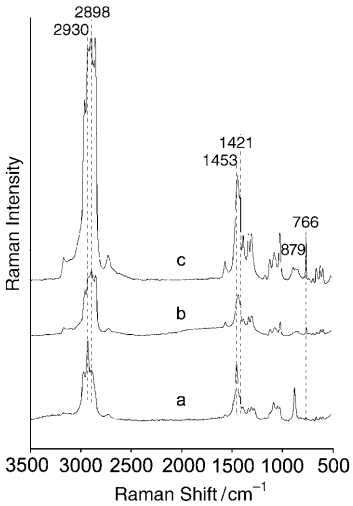

Figure 9. FT-Raman spectra of a) 17 wt% $DMImBF_4$/silica gel, b) 17 wt% $DMImBF_4/SiO_2$, and c) pure $DMImBF_4$ ionic liquid.

The transformation reaction of cyclohexanone oxime and acetone[45] can be catalyzed with ionic liquids. Only 22.5% of conversion was achieved when the bulk ionic liquid $DMImBF_4$ was used as catalyst directly and similar results were obtained if a physical mixture of pure silica gel and the ionic liquid $DMImBF_4$ was used (Table 4, entries 1 and 2). Surprisingly, more than 90% of conversions with nearly 100% of selectivity were achieved when using 17 wt% $DMImBF_4$/silica gel as catalyst (Table 4, entry 3), for which the TOFs were 16–27 times higher than that of

Table 3. Results of oxidative carbonylation of aniline to phenyl carbamate in methanol.

	Catalyst	Ionic liquid/ metal complex [mg]	Conv [%]	Sel [%]	TOF
1	$[Pd(PPh_3)_2Cl_2]$–$DMImBF_4$	2500/1	13	>99	494
2	$[Rh(PPh_3)_3Cl]$–$DMImBF_4$	2500/1	15	96	752
3	0.15 wt% Pd–35 wt% $DMImBF_4$/silica gel	~35/~1	63	>98	2650
4	0.11 wt% Rh–35 wt% $DMImBF_4$/silica gel	~35/~1	89	>98	4960

Table 4. Results of C=N and C=O bond exchange between cyclohexanone oxime and acetone.

	Catalyst	Ionic liquid [mg]	Conv [%]	Sel [%]	TOF
1	$DMImBF_4$	10	22.5	>99	6
2	$DMImBF_4$ + silica gel	10	22	>99	6
3	17 wt% $DMImBF_4$/silica gel	~1.7	92.1	>99	100
4	17 wt% $DMImBF_4/SiO_2$	~1.7	24.7	>99	27

 © 2005 Wiley-VCH Verlag GmbH & Co. KGaA, Weinheim

the bulk ionic-liquid catalyst. If 17 wt % $DMImBF_4/SiO_2$ was used as the catalyst for the transformation reaction of cyclohexanone oxime and acetone, only 24.7 % of conversion was obtained (Table 4, entry 4); this also showed the silica-gel-confined ionic liquid was more effective than the bulk or silica-supported ionic liquid as catalysts. Both the results of the carbonylation reaction and oxime transformation also confirmed that higher catalytic activities could be exhibited with silica-gel-confined ionic-liquid nanocatalyst systems. These results further confirmed that the enhancement in catalytic activities may be derived from the formation of nanoscale and high-concentration ionic liquids due to the confinement in the nanopores of silica gel, in which the restrictive dimensions of the silica gel interior may force unusual compound symmetry, coordination geometry, and coordinative unsaturation upon the entrapped ionic liquid and metal complex, rather than being related to the use of a support to improve the possible transport restrictions occurring in bulk ionic liquid. As a matter of fact, the problem of mass transfer may indeed occur when the bulk ionic liquids are immobilized into a porous support.

Conclusion

In summary, physically confined ionic liquids on the nanoscale, with or without a metal complex, in silica gel were developed through a "one-pot" sol–gel method as a new kind of supported nanoliquid catalyst. The confined ionic liquids on the nanoscale exhibited abnormal Raman spectra, and particularly important was that they exhibited greatly enhanced catalytic performance with less ionic liquid required relative to the bulk and pure ionic liquids. The preliminary investigations showed that such silica-gel-confined ionic-liquid catalysts may be effective for a wider range of reactions. The preparation of these supported nanoliquid catalysts could be further optimized and modified, and their application expanded to other reactions and processes.

Experimental Section

Ionic liquids and metal complex synthesis: All chemicals used were analytical grade and used without further purification. The ionic liquids used in this work were synthesized according to the literature.[46,47] Two kinds of typical ionic liquids, in which the cations and anions were dialkyl imidazolium and BF_4^- and PF_6^-, respectively, were employed for the synthesis of silica-gel-confined ionic-liquid catalysts:

The two metal complexes employed, $[Pd(PPh_3)_2Cl_2]$ and $[Rh(PPh_3)_3Cl]$, were synthesized according to the literature.[48,49]

Synthesis of silica-gel-confined ionic-liquid catalysts: A mixture of tetraethoxyorthosilicate (TEOS, 10 mL) and EtOH (7 mL) was heated to 60 °C and then ionic liquids (0.2–4 g) or ionic-liquids (2 g) containing $[Pd(PPh_3)_2Cl_2]$ or $[Rh(PPh_3)_3Cl]$ (50 mg) were immediately transferred into the TEOS. After the formation of a clear and homogeneous liquid mixture, hydrochloric acid (5 M, 5 mL) was added and the mixture gradually coagulated. After aging at 60 °C for 12 h, the resultant solid material was dried in vacuum at 150 °C for 3 h and 3–7 g of solid sample was obtained. It is worth noting that a dry solid sample of silica-gel-confined ionic liquid was obtained even with ionic liquid loading of up to 53 wt %, indicating that the ionic liquid added could be completely encapsulated into sol–gel. Therefore, the loadings of confined ionic liquids could be calculated according to the weight of ionic liquids added originally. Solid samples exhibited different colors depending on the different ionic liquids, their loadings, and on whether they contained metal complex or not (Figure 10).

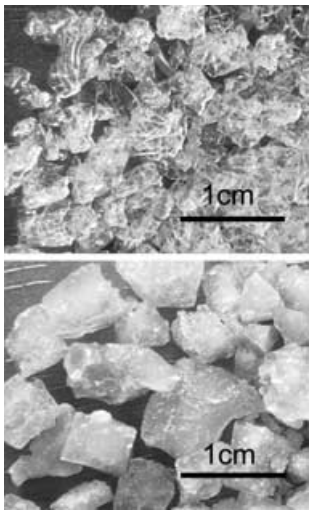

Figure 10. Two kinds of typical silica-gel-confined ionic liquid samples: 53 wt % $BuMImBF_4$/silica gel (top) and 0.11 wt % Rh-35wt % $DMImBF_4$/silica gel (bottom).

A series of samples of silica-gel-confined ionic liquids (either with or without $[Pd(PPh_3)_2Cl_2]$ and $[Rh(PPh_3)_3Cl]$) and with various ionic liquid or metal loadings were denoted as follows: $BuMImBF_4$: 8 wt % $BuMImBF_4$/silica gel, 17 wt % $BuMImBF_4$/silica gel, 35 wt % $BuMImBF_4$/silica gel, 53 wt % $BuMImBF_4$/silica gel; $DMImBF_4$: 8 wt % $DMImBF_4$/silica gel, 17 wt % $DMImBF_4$/silica gel, 35 wt % $DMImBF_4$/silica gel, 53 wt % $DMImBF_4$/silica gel; $EMImBF_4$: 17 wt % $EMImBF_4$/silica gel; $CMImBF_4$: 17 wt % $CMImBF_4$/silica gel; 0.15 wt % Pd-35 wt % $DMImBF_4$/silica gel, 0.11 wt % Rh-35 wt % $DMImBF_4$/silica gel, 0.13 wt % Rh-35 wt % $EMImBF_4$/silica gel.

Synthesis of SiO_2-supported ionic-liquid catalysts: For the purpose of comparison, synthesis and catalytic performance of SiO_2-supported ionic liquid as catalysts, in which the ionic liquid was deposited as a thin layer on the support, were also conducted. SiO_2 pellets (4.9 g, ∅ 0.5–0.6 mm, average pore diameter: 52 Å, pore volume: 0.75 mL g^{-1}, surface area: 578 $m^2 g^{-1}$) calcined at 400 °C for 6 h, were charged into a 50 mL three-necked round-bottomed flask. Under the conditions of vacuum (approximately 5 mm Hg) and room temperature, solutions of $DMImBF_4$ ionic liquid (1 g, or 2.7 g $DMImBF_4$ ionic liquid containing 70 mg $[Rh(PPh_3)_3Cl]$) and ethanol (6 mL) were transferred into the flask, and the adsorption/absorption was conducted for 1 h. The resultant catalyst precursors were then dried under vacuum (approximately 5 mm Hg) at 150 °C for another 4 h to remove the residual ethanol completely. Two kinds of silica-supported ionic liquids (with and without $[Rh(PPh_3)_3Cl]$) were denoted as follows: 17 wt % $DMImBF_4/SiO_2$; 0.11 wt % Rh-35wt % $DMImBF_4/SiO_2$.

Catalyst sample characterization: FT-Raman analysis was conducted with a Nicolet 910 Raman spectrometer. Only the samples of silica-gel-confined ionic liquid without metal complexes were characterized, because the loadings of metal complexes were too low to be observed in the FT-Raman spectra.

BET surface areas (S_{BET}) were obtained by physisorption of N_2 at 77 K by using a Micromeritics ASAP 2020. Prior to measurement, samples were degassed to 0.1 Pa at 373 K.

© 2005 Wiley-VCH Verlag GmbH & Co. KGaA, Weinheim

TEM analysis was performed on a JEOL JEM-100CXII transmission electron microscope. The specimens for electron microscopy were prepared by gently grinding the powder samples suspended in ethanol in an agate mortar, and then the resultant solution was dropped onto the carbon film of the copper grid.

XRD was performed on a Philips X'Pert Pro powder X-ray diffractometer.

The metal Rh or Pd in the samples of silica-gel-confined ionic liquids were analyzed with a 3520 ICT AES instrument (ARL Co. USA).

Synthesis of diphenyl urea:

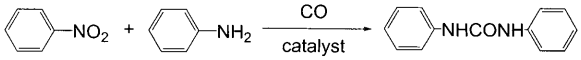

The carbonylation of aniline and nitrobenzene for the synthesis of diphenyl urea was conducted as follows: Pd(or Rh)-EMImBF$_4$/silica gel or Pd(or Rh)-DMImBF$_4$/silica gel (0.1 g, 50–60 mesh), or DMImBF$_4$ ionic liquid (2.5 g) containing Rh complex (1 mg), or 0.11 wt % Rh-35 wt % DMImBF$_4$/SiO$_2$ (0.1 g, for the purpose of comparison), nitrobenzene (10 mmol), aniline (10 mmol), and CO gas (5.0 MPa, purity 99.99 %) were successively introduced into an autoclave (90 mL) without any additional organic solvent. The reaction proceeded at 180 °C for 1.5 h and then was cooled to room temperature. Since the desired diphenyl urea was insoluble in methanol and water, methanol (20 mL) was added to the resultant solid mixture (if the conversion and selectivity was enough high) to dissolve the unreacted substrates for analysis and, hence, obtain the conversion of nitrobenzene and aniline by means of GC with an outstandard method. Then, filtration was conducted to remove methanol, and water (20 mL) was added to the solid mixture containing diphenyl urea and the catalyst. The diphenyl urea floated on the water and the catalyst deposited on the bottom. They could be easily separated with a simple dredge and filtration method, and the isolated yield of diphenyl urea was obtained. The catalyst could be reused after drying. The selectivity was calculated as follows: selectivity (%) = isolated yield/conversion × 100 %.

Synthesis of phenyl carbamate:

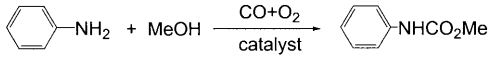

The carbonylation of aniline for synthesis of carbamates was conducted as follows: Pd(or Rh)-DMImBF$_4$/silica gel (0.1 g, 50–60 mesh), or DMImBF$_4$ ionic liquid (2.5 g) containing Pd(or Rh) complex (1 mg, for the purpose of comparison), aniline (0.5 mL), methanol (5 mL) and a CO/O$_2$ gas mixture (5.0 MPa: CO purity 99.99 % 4.5 MPa and O$_2$ 99.99 % purity 0.5 MPa) were successively introduced into an autoclave (90 mL) without any additional organic solvent. The reaction proceeded at 135 °C for 1 h and the autoclave was then cooled to room temperature, and methanol (20 mL) was added to dissolve the resultant mixture for analyses.

Oxime transformation between cyclohexanone oxime and acetone:

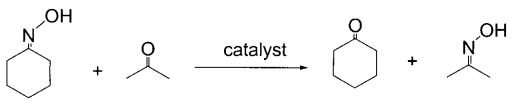

The oxime transformation between cyclohexanone oxime and acetone was carried out as follows: cyclohexanone oxime (0.2 g), 17 wt % DMImBF$_4$/silica gel (0.01 g, 50–60 mesh) or pure DMImBF$_4$ ionic liquid (0.01 g) or 17wt % DMImBF$_4$/SiO$_2$ (0.01 g, for the purpose of comparison), acetone (2 mL) and water (6 mL) were successively added into a 25 mL round-bottomed flask and the mixture was stirred magnetically at room temperature (approximately 20 °C) for 2 h. Then, the resultant solution containing reactants and products was directly analyzed without further treatment.

Analyses: Qualitative analyses were conducted with a HP 6890/5973 GC-MS with a 30 m × 0.25 mm × 0.33 μm capillary column and a chemstation containing a NIST Mass Spectral Database. Quantitative analyses were conducted with a Agilent (Shanghai) 1790 GC equipped with FID detector and 30 m × 0.25 mm × 0.33 μm capillary column.

Acknowledgement

This work was financially supported by the National Natural Science Foundation of China (No. 20233040 and No. 20225309).

[1] Y. Wada, *Surf. Sci.* **1997**, *386*, 276.
[2] R. Bauer, G. Waldner, S. Fallmann, S. Hager, T. Krutzler, S. Malato, P. Maletzky, *Catal. Today* **1999**, *53*, 131.
[3] C. B. Geoffrey, T. T. David, *Catal. Rev.* **1999**, 319.
[4] S. Miao, Y. Deng, *Appl. Catal. B.* **2001**, *31*, L1.
[5] F. Shi, Y. Deng, T. SiMa, H. Yang, *J. Catal.* **2002**, *211*, 548.
[6] J. Jortner, *Z. Phys. Chem.* **1994**, *184*, 283.
[7] P. Alivisatos, *Science* **1996**, *271*, 933.
[8] I. Last, J. Jorter, *Phys. Rev. Lett.* **2001**, *87*, 3401.
[9] J. Dupont, G. S. Fonseca, A. P. Umpierre, P. F. P. Fichtner, S. R. Teixeira, *J. Am. Chem. Soc.* **2002**, *124*, 4228.
[10] V. Calo, A. Nacci, A. Monopoli, S. Laera, N. Cioffi, *J. Org. Chem.* **2003**, *68*, 2929.
[11] D. Zhao, Z. Fei, T. J. Geldbach, R. Scopelliti, P. J. Dyson, *J. Am. Chem. Soc.* **2004**, *126*, 15876.
[12] K. He, Z. Zhou, L. Wang, K. Li, G. Zhao, Q. Zhou, C. Tang, *Synlett* **2004**, *9*, 1525.
[13] L. M. Rossi, G. Machado, P. F. P. Fichtner, S. R. Teixeira, J. Dupont, *Catal. Lett.* **2004**, *92*, 149.
[14] K. Anderson, S. C. Fernández, C. Hardacre, P. C. Marr, *Inorg. Chem. Commun.* **2004**, *7*, 73.
[15] J. Huang, T. Jiang, B. Han, H. Gao, Y. Chang, G. Zhao, W. Wu, *Chem. Commun.* **2003**, 1654.
[16] E. T. Silveira, A. P. Umpierre, L. M. Rossi, G. Machado, J. Morais, G. V. Soares, I. J. R. Baumvol, S. R. Teixeira, P. F. P. Fichtner, J. Dupont, *Chem. Eur. J.* **2004**, *10*, 3734.
[17] W. Liu, A. G. Fadeev, B. Qi, E. Smela, B. R. Mattes, J. Ding, G. M. Spinks, J. Mazurkiewicz, D. Zhou, G. G. Wallace, D. R. MacFarlane, S. A. Forsyth, M. Forsyth, *Science* **2002**, *297*, 983.
[18] J. Dupont, R. F. de Souza, P. A. Z. Suarez, *Chem. Rev.* **2002**, *102*, 3667.
[19] P. Wasserscheid, W. Keim, *Angew. Chem.* **2000**, *112*, 3926; *Angew. Chem. Int. Ed.* **2000**, *39*, 3772.
[20] T. Welton, *Chem. Rev.* **1999**, *99*, 2071.
[21] W. Chen, L. Xu, C. Chatterton, J. Xiao, *Chem. Commun.* **1999**, 1247.
[22] B. Ellis, W. Keim, P. Wasserscheid, *Chem. Commun.* **1999**, 337.
[23] J. Peng, Y. Deng, *New J. Chem.* **2001**, *25*, 639.
[24] J. Peng, Y. Deng, *Tetrahedron Lett.* **2001**, *42*, 403.
[25] J. Peng, Y. Deng, *Tetrahedron Lett.* **2001**, *42*, 5917.
[26] M. Antonietti, D. Kuang, B. Smarsly, Y. Zhou, *Angew. Chem.* **2004**, *116*, 5096; *Angew. Chem. Int. Ed.* **2004**, *43*, 4988.
[27] J. Dupont, *J. Braz. Chem. Soc.* **2004**, *15*, 341.
[28] C. P. Mehnert, R. A. Cook, N. C. Dispenziere, M. Afeworki, *J. Am. Chem. Soc.* **2002**, *124*, 12932.
[29] M. H. Valkenberg, C. deCastro, W. F. Hölderich, *Green Chem.* **2002**, *4*, 88.
[30] H. Hagiwara, Y. Sugawara, K. Isobe, T. Hoshi, T, Suzuki, *Org. Lett.* **2004**, *6*, 2325.
[31] A. Elaiwi, P. B. Hitchcock, K. R. Seddon, N. Srinivasan, Y. Tan, T. Welton, J. A. Zora, *J. Chem. Soc. Dalton Trans.* **1995**, 3467.
[32] N. Nanbu, Y. Sasaki, F. Kitamura, *Electrochem. Commun.* **2003**, *5*, 383.
[33] C. Perchard, A. Novak, *Spectrochim. Acta A* **1967**, *23*, 1953.

 © 2005 Wiley-VCH Verlag GmbH & Co. KGaA, Weinheim

[34] M. Majoube, M. Henry, L. Chinsky, P. Y. Turpin, *Chem. Phys.* **1993**, *169*, 231.
[35] D. Garfinkel, J. T. Edsall, *J. Am. Chem. Soc.* **1958**, *80*, 3807.
[36] A. Toyama, K. Ono, S. Hashimoto, H. Takeuchi, *J. Phys. Chem. A.* **2002**, *106*, 3403.
[37] S. L. Burkett, S. D. Sims, S. Mann, *Chem. Commun.* **1996**, 1367.
[38] N. Herron, G. D. Stucky, C. A. Tolman, *Inorg. Chim. Acta* **1986**, *25*, 4717.
[39] M. Ichikawa, T. Kimura, A. Fukuoka, *Stud. Surf. Sci. Catal.* **1991**, *60*, 335.
[40] B. V. Romanovsky, A. G. Gabrielov, *J. Mol. Catal.* **1992**, *74*, 293.
[41] S. Kowalak, R. C. Weiss, K. J. Balkus Jr., *J. Chem. Soc. Chem. Commun.* **1991**, 57.
[42] V. L. K. Valli, H. Alper, *J. Am. Chem. Soc.* **1993**, *115*, 3778.
[43] I. Pri-Bar and J. Schwartz, *J. Org. Chem.* **1995**, *60*, 8124.
[44] F. Shi, J. Peng, Y. Deng, *J. Catal.* **2003**, *219*, 372.
[45] D. Li, F. Shi, S. Guo, Y. Deng, *Tetrahedron Lett.* **2004**, *45*, 265.
[46] P. Bonhote, A. P. Dias, N. Papageorgiou, K. Kalyanasundaram, M. Grätzel, *Inorg. Chem.* **1996**, *35*, 1168.
[47] P. A. Z. Suarez, J. E. L. Dullius, S. Einloft, R. F. de Souza, J. Dupont, *Polyhedron*, **1996**, *15*, 1217.
[48] H. Itatani, J. C. Bailar Jr., *J. Am. Oil Chem. Soc.* **1967**, *44*, 147.
[49] T. A. Stepheson, G. Wilkison, *J. Inorg. Nucl. Chem.* **1966**, *28*, 945.

Received: January 29, 2005
Published online: July 4, 2005

© 2005 Wiley-VCH Verlag GmbH & Co. KGaA, Weinheim